Supplementary Material of:

Robust historical evapotranspiration trends across climate regimes

Sanaa Hobeichi[1,2], Gab Abramowitz[1,2], and Jason Evans[1,2]

[1] Climate Change Research Centre, UNSW Sydney, NSW 2052, Australia.

[2]ARC Centre of Excellence for Climate Extremes, UNSW Sydney, NSW 2052, Australia.

Correspondence to: Sanaa Hobeichi (s.hobeichi@unsw.edu.au)

S1. Flux tower data

Table S1: Observational data used to constrained the weighting and/or validate DOLCE V2. Site data was accessed during July – November, 2019. Data source includes Ameriflux (ameriflux.lbl.gov), the Atmospheric Radiation Measurement (ARM; arm.gov), AsiaFlux (asiaflux.net), European Fluxes Database (europe-fluxdata.eu), Fluxnet 2015, LaThuile Free Fair Use (fluxnet.fluxdata.org), Oak Ridge data repository (daac.ornl.gov), OzFlux (ozflux.org.au) and individual site principal investigators (PI).

Site ID	Country	Longitude	Latitude	Data source	Reference
AR-SLu	Argentina	-66.4598	-33.4648	Fluxnet 2015	(Cleverly et al., 2013)
AT-Neu	Austria	11.3175	47.11667	Fluxnet 2015	(Cleverly et al., 2013)
AU-Ade	Australia	131.1178	-13.0769	Fluxnet 2015	(Beringer, 2013a)
AU-ASM	Australia	133.249	-22.283	Fluxnet 2015	(Cleverly et al., 2013)
AU-Cum	Australia	150.7225	-33.6133	Fluxnet 2015	(Pendall, 2015)
AU-CPr	Australia	140.5891	-34.0021	OzFlux	(Calperum Tech, 2013)
AU-CTr	Australia	145.4469	-16.1032	OzFlux	(Liddell, 2013a)
AU-DaS	Australia	131.388	-14.1593	Fluxnet 2015	(Isaac, 2010)
AU-Dry	Australia	132.3706	-15.2588	Fluxnet 2015	(Beringer, 2013b)
AU-Emr	Australia	148.4746	-23.8587	Fluxnet 2015	(Schroder, 2014)
AU-Fog	Australia	131.3072	-12.5452	Fluxnet 2015	(Beringer, 2013c)
AU-How	Australia	131.1523	-12.4943	OzFlux	(Andrykanus, 2012)
AU-Gin	Australia	115.65	-31.375	Fluxnet 2015	(Silberstein, 2015)
AU-GWW	Australia	120.6542	-30.1914	OzFlux	(Macfarlane, 2013)
AU-Lox	Australia	140.6551	-34.4704	Fluxnet 2015	(Ewenz, 2015)

AU-RDF	Australia	132.4776	-14.5636	Fluxnet 2015	(Beringer, 2014a)
AU-Rig	Australia	145.576	-36.656	Fluxnet 2015	(Beringer, 2014a)
AU-Rob	Australia	145.6302	-17.1174	Fluxnet 2015	(Liddell, 2013b)
AU-Stp	Australia	133.3503	-17.1508	Fluxnet 2015	(Beringer, 2013d)
AU-TTE	Australia	133.64	-22.287	Fluxnet 2015	(Cleverly, 2013)
AU-Tum	Australia	148.1516	-35.6566	Fluxnet 2015	(Woodgate, 2013)
AU-Ync	Australia	146.2907	-34.9893	OzFlux	(Beringer, 2013e)
AU-Wac	Australia	145.1873	-37.429	Fluxnet 2015	(Beringer, 2013f)
AU-Whr	Australia	145.0294	-36.6732	OzFlux	(Beringer, 2017)
AU-Wom	Australia	144.0944	-37.4222	Fluxnet 2015	(Stefan, 2013)
BE-Bra	Belgium	4.52056	51.30917	Fluxnet 2015	(Stoy et al., 2013)
BE-Lon	Belgium	4.74613	50.55159	Fluxnet 2015	(McCaughey et al., 2006)
BE-Vie	Belgium	5.99805	50.30507	Fluxnet 2015	(Stoy et al., 2013)
BNS	China	101.2653	21.9275	AsiaFlux	asiaflux.net
BR-Ban	Brazil	-50.1591	-9.82442	Oak Ridge	(Saleska et al., 2013)
BR-Ji1	Brazil	-62.3572	-10.7618	Oak Ridge	(Saleska et al., 2013)
BR-Ji3	Brazil	-61.9331	-10.078	Oak Ridge	(Saleska et al., 2013)
BR-Ma2	Brazil	-60.2091	-2.609	Oak Ridge	(Saleska et al., 2013)
BR-Sa1	Brazil	-54.959	-2.857	Oak Ridge	(Saleska et al., 2013)
BR-Sa3	Brazil	-54.9714	-3.01803	LaThuile	(Stoy et al., 2013)
BW-Ma1	Botswana	23.56033	-19.9165	LaThuile	(Stoy et al., 2013)
CA-ARF	Canada	-83.955	52.7008	AmeriFlux	(Euskirchen et al., 2017)
CA-Ca2	Canada	-125.291	49.8705	AmeriFlux	(Chen et al., 2006)
CA-Cbo	Canada	-79.9333	44.3167	AmeriFlux	(Barr et al., 2002)
CA-Ca3	Canada	-124.9	49.5346	AmeriFlux	(Chen et al., 2006)
CA-Let	Canada	-112.94	49.7093	AmeriFlux	(Conte et al., 2003)
CA-Man	Canada	-98.4808	55.8796	LaThuile	fluxnet.ornl.gov
CA-Mer	Canada	-75.5186	45.4094	LaThuile	(Lafleur, et al., 2003)
CA-NS2	Canada	-98.5247	55.9058	LaThuile	fluxnet.ornl.gov
CA-NS6	Canada	-98.9644	55.9167	LaThuile	fluxnet.ornl.gov
CA-NS7	Canada	-99.9483	56.6358	LaThuile	fluxnet.ornl.gov
CA-Ojp	Canada	-104.692	53.9163	AmeriFlux	(Baldocchi et al., 2000)
CA-Qcu	Canada	-74.0365	49.2671	LaThuile	(Chu et al., 2018)
CA-Qfo	Canada	-74.3421	49.6925	Fluxnet 2015	fluxnet.ornl.gov
CA-SCC	Canada	-121.299	61.3079	AmeriFlux	(Euskirchen et al., 2017)
CA-SF1	Canada	-105.818	54.485	Fluxnet 2015	fluxnet.ornl.gov
CA-SF3	Canada	-106.005	54.0916	Fluxnet 2015	fluxnet.ornl.gov
CA-TP1	Canada	-80.5595	42.6609	AmeriFlux	(Arain et al., 2005)
CA-TP4	Canada	-80.3574	42.7102	AmeriFlux	(Arain et al., 2005)
CH-Cha	Switzerland	8.41044	47.21022	Fluxnet 2015	fluxnet.ornl.gov
CH-Dav	Switzerland	9.85592	46.81533	Fluxnet 2015	fluxnet.ornl.gov

CH-Fru	Switzerland	8.53778	47.11583	Fluxnet 2015	fluxnet.ornl.gov
CH-Oe1	Switzerland	7.73194	47.28583	LaThuile	fluxnet.ornl.gov
CN-Cng	China	123.5092	44.5934	Fluxnet 2015	fluxnet.ornl.gov
CN-Du2	China	116.2836	42.0467	Fluxnet 2015	(Stoy et al., 2013)
CN-HaM	China	101.18	37.37	Fluxnet 2015	(Li et al., 2013)
CN-QHB	China	101.332	37.60743	AsiaFlux	asiaflux.net
CN-QYZ	China	115.0663	26.73396	AsiaFlux	asiaflux.net
CZ-BK1	Czech Republic	18.53688	49.50208	European Fluxes DB	europe-fluxdata.eu
CZ-BK2	Czech Republic	18.54285	49.49443	European Fluxes DB	europe-fluxdata.eu
CZ-RAJ	Czech Republic	16.69651	49.44372	European Fluxes DB	europe-fluxdata.eu
CZ-Stn	Czech Republic	17.9699	49.03598	European Fluxes DB	europe-fluxdata.eu
CZ-wet	Czech Republic	14.77035	49.02465	Fluxnet 2015	(Stoy et al., 2013)
DE-Geb	Germany	10.9143	51.1001	Fluxnet 2015	(Revill et al., 2013)
DE-Hai	Germany	10.453	51.07917	Fluxnet 2015	(Ershadi et al., 2014)
DE-Hte	Germany	12.17611	54.21028	European Fluxes DB	europe-fluxdata.eu
DE-Hzd	Germany	13.48982	50.96403	European Fluxes DB	europe-fluxdata.eu
DE-Kli	Germany	13.52251	50.89288	Fluxnet 2015	(Revill et al., 2013)
DE-Lkb	Czech Republic	13.30467	49.09962	Fluxnet 2015	fluxnet.ornl.gov
DE-Meh	Germany	10.65547	51.27531	LaThuile	fluxnet.ornl.gov
DE-RuR	Germany	6.30413	50.62191	Fluxnet 2015	fluxnet.ornl.gov
DE-Seh	Germany	6.44965	50.87062	Fluxnet 2015	fluxnet.ornl.gov
DE-SfN	Germany	11.3275	47.80639	Fluxnet 2015	fluxnet.ornl.gov
DE-Wet	Germany	11.45753	50.4535	LaThuile	(Stoy et al., 2013)
DE-Zrk	Germany	12.88901	53.87594	Fluxnet 2015	fluxnet.ornl.gov
DK-Fou	Denmark	9.58722	56.4842	LaThuile	(Stoy et al., 2013)
DK-Ris	Denmark	12.09722	55.53028	LaThuile	(Gilmanov et al., 2010)
DK-Sor	Denmark	11.64464	55.48587	Fluxnet 2015	(Stoy et al., 2013)
DK-ZaF	Greenland	-20.5557	74.4791	Fluxnet 2015	(Soegaard and Nordstroem, 1999)
ES-ES1	Spain	-0.31881	39.34597	LaThuile	(Stoy et al., 2013)
ES-LgS	Spain	-2.96583	37.09794	Fluxnet 2015	fluxnet.ornl.gov
ES-LJu	Spain	-2.75212	36.92659	Fluxnet 2015	fluxnet.ornl.gov
ES-LMa	Spain	-5.77336	39.9415	LaThuile	(Stoy et al., 2013)
ES-VDA	Spain	1.4485	42.15218	LaThuile	(Stoy et al., 2013)
FI-Hyy	Finland	24.295	61.8475	Fluxnet 2015	(Stoy et al., 2013)
FI-Jok	Finland	23.51345	60.8986	Fluxnet 2015	(Reichstein et al., 2005)
FI-Kaa	Finland	27.29503	69.14069	LaThuile	(Aurela et al., 2001)
FI-Kns	Finland	24.35617	60.64683	European Fluxes DB	europe-fluxdata.eu
FI-Lom	Finland	24.20918	67.9972	Fluxnet 2015	fluxnet.ornl.gov

FI-Sod	Finland	26.63783	67.36186	Fluxnet 2015	(Stoy et al., 2013)
FI-Var	Finland	29.61	67.7549	European Fluxes DB	europe-fluxdata.eu
FR-Fon	France	2.78014	48.4764	LaThuile	(Stoy et al., 2013)
FR-Gri	France	1.95191	48.84422	Fluxnet 2015	(Loubet et al., 2011)
FR-Hes	France	7.06556	48.67416	LaThuile	(Reichstein et al., 2005)
FR-LBr	France	-0.7693	44.71711	Fluxnet 2015	fluxnet.ornl.gov
FR-Lq1	France	2.73583	45.64306	LaThuile	(Gilmanov et al., 2007)
FR-Lq2	France	2.73703	45.63919	LaThuile	(Gilmanov et al., 2007)
FR-Lus	France	0.12065	46.41425	European Fluxes DB	europe-fluxdata.eu
FR-Pue	France	3.59583	43.74139	Fluxnet 2015	(Wei et al., 2014)
GRW	Portugal	-28.0297	39.0911	ARM	(ARM, 2009)
HFE	China	116.782	32.5584	ARM	(ARM, 2008)
HFK	S.Korea	127.57	34.55389	AsiaFlux	asiaflux.net
HU-He1	Hungary	16.65222	46.95583	PI	(Barcza et al., 2009)
HU-Bug	Hungary	19.6013	46.6911	LaThuile	(Stoy et al., 2013)
HU-Mat	Hungary	19.726	47.8469	LaThuile	(Stoy et al., 2013)
ID-Pag	Malaysia	114.036	2.345	LaThuile	(Hirano et al., 2007)
IE-Ca1	Ireland	-6.91814	52.85879	LaThuile	(Stoy et al., 2013)
IE-Dri	Ireland	-8.75181	51.98669	LaThuile	(Stoy et al., 2013)
IL-Yat	Israel	35.0515	31.345	LaThuile	(Reichstein et al., 2003)
IS-Gun	Iceland	-20.2167	63.8333	LaThuile	fluxnet.ornl.gov
IT-BCi	Italy	14.95744	40.52375	Fluxnet 2015	fluxnet.ornl.gov
IT-CA3	Italy	12.0222	42.38	Fluxnet 2015	fluxnet.ornl.gov
IT-Cas	Italy	8.71752	45.07005	LaThuile	fluxnet.ornl.gov
IT-Col	Italy	13.58814	41.84936	Fluxnet 2015	(Stoy et al., 2013)
IT-Cpz	Italy	12.37611	41.70525	Fluxnet 2015	(Wei et al., 2014)
IT-Isp	Italy	8.63358	45.81264	Fluxnet 2015	fluxnet.ornl.gov
IT-Lav	Italy	11.28132	45.9562	Fluxnet 2015	(Cescatti and Zorer, 2003)
IT-Lec	Italy	11.26975	43.30359	LaThuile	(Stoy et al., 2013)
IT-LMa	Italy	7.58259	45.15258	LaThuile	fluxnet.ornl.gov
IT-Mal	Italy	11.70334	46.11402	LaThuile	(Gilmanov et al., 2007)
IT-MBo	Italy	11.04583	46.01468	Fluxnet 2015	(Gilmanov et al., 2007)
IT-Noe	Italy	8.15146	40.60613	Fluxnet 2015	fluxnet.ornl.gov
IT-Non	Italy	11.09109	44.69019	LaThuile	fluxnet.ornl.gov
IT-PT1	Italy	9.06104	45.20087	Fluxnet 2015	(Stoy et al., 2013)
IT-Ren	Italy	11.43369	46.58686	Fluxnet 2015	(Stoy et al., 2013)
IT-Ro3	Italy	11.91542	42.37539	European Fluxes DB	europe-fluxdata.eu
IT-SRo	Italy	10.28444	43.72786	Fluxnet 2015	fluxnet.ornl.gov
IT-Tor	Italy	7.57806	45.84444	Fluxnet 2015	(Galvagno et al., 2013)
JP-TKY	Japan	137.4231	36.14617	AsiaFlux	(Hirata et al., 2008)
MAO	Brazil	-60.5981	-3.21297	ARM	(ARM, 2014)

MMF	Japan	142.2613	44.3219	AsiaFlux	asiaflux.net
MN-SKT	Mongolia	108.6543	48.35186	AsiaFlux	(Hirata et al., 2008)
MSE	Japan	140.0269	36.054	AsiaFlux	asiaflux.net
MX-Lpa	Mexico	-110.438	24.1293	AmeriFlux	(Bell et al., 2012)
NIM	Niger	2.1758	13.4773	ARM	(ARM, 2005)
NL-Ca1	Netherlands	4.927	51.971	LaThuile	fluxnet.ornl.gov
NL-Haa	Netherlands	4.80556	52.00361	LaThuile	fluxnet.ornl.gov
NL-Hor	Netherlands	5.0713	52.24035	Fluxnet 2015	(Sulkava et al., 2011)
NL-Loo	Netherlands	5.74356	52.16658	Fluxnet 2015	(Gash and Dolman, 2003)
NL-Mol	Netherlands	4.63908	51.65	LaThuile	(Gilmanov et al., 2007)
NO-Adv	Norway	15.923	78.186	Fluxnet 2015	fluxnet.ornl.gov
NSA	USA	-156.608	71.325	ARM	(ARM, 2011)
NZ-BFu	New Zealand	171.9268	-43.5918	OzFlux	(Laubach, 2016)
PL-wet	Poland	16.3094	52.7622	LaThuile	(stoy et al., 2013)
PT-Esp	Portugal	-8.6018	38.6394	LaThuile	(stoy et al., 2013)
PT-Mi1	Portugal	-8.00006	38.54064	LaThuile	(stoy et al., 2013)
PT-Mi2	Portugal	-8.02455	38.4765	LaThuile	(stoy et al., 2013)
RU-Cok	Russia	147.4943	70.82914	Fluxnet 2015	(Stoy et al., 2013)
RU-Fyo	Russia	32.92208	56.46153	Fluxnet 2015	(Stoy et al., 2013)
RU-Ha1	Russia	90.00215	54.72517	Fluxnet 2015	(Belelli Marchesini et al., 2007)
RU-Ha2	Russia	89.95664	54.77301	LaThuile	(Belelli Marchesini et al., 2007)
RU-Ha3	Russia	89.07785	54.70455	LaThuile	(Belelli Marchesini et al., 2007)
RU-Zot	Russia	89.3508	60.8008	LaThuile	(Eugster et al., 2000)
SD-Dem	Sudan	30.4783	13.2829	Fluxnet 2015	fluxnet.ornl.gov
SE-Deg	Sweden	19.55669	64.18197	LaThuile	fluxnet.ornl.gov
SE-Faj	Sweden	13.55351	56.26547	LaThuile	(Stoy et al., 2013)
SE-Fla	Sweden	19.45694	64.11278	LaThuile	(Stoy et al., 2013)
SE-Nor	Sweden	17.4795	60.0865	LaThuile	(Stoy et al., 2013)
SE-Sk2	Sweden	17.84006	60.12967	LaThuile	(Stoy et al., 2013)
SE-Svb	Sweden	19.7745	64.25611	European Fluxes DB	europe-fluxdata.eu
SGP	USA	-96.855	37.521	ARM	(ARM, 1997)
SN-Dhr	Senegal	-15.4322	15.40278	Fluxnet 2015	fluxnet.ornl.gov
TWP	Australia	130.881	-12.486	ARM	(ARM, 2013)
UK-EBu	UK	-3.20578	55.866	LaThuile	(Stoy et al., 2013)
UK-ESa	UK	-2.85861	55.90694	LaThuile	(Stoy et al., 2013)
UK-Gri	UK	-3.79806	56.60722	LaThuile	(Stoy et al., 2013)
UK-Ham	UK	-0.8583	51.15353	LaThuile	(Stoy et al., 2013)
UK-LBT	UK	-0.1389	51.5215	European Fluxes DB	europe-fluxdata.eu
UK-PL3	UK	-1.26667	51.45	LaThuile	fluxnet.ornl.gov
UK-Tad	UK	-2.82864	51.2071	LaThuile	fluxnet.ornl.gov
US-ADR	USA	-116.693	36.7653	AmeriFlux	(Euskirchen et al., 2017)
US-AR1	USA	-99.42	36.4267	Fluxnet 2015	fluxnet.ornl.gov

US-AR2	USA	-99.5975	36.6358	Fluxnet 2015	fluxnet.ornl.gov
US-ARc	USA	-98.0401	35.54649	Fluxnet 2015	(Stoy et al., 2013)
US-ARM	USA	-97.4888	36.6058	Fluxnet 2015	(Bagley et al., 2017)
US-Aud	USA	-110.51	31.5907	AmeriFlux	(Baldocchi et al., 2015)
US-Bar	USA	-71.2881	44.0646	LaThuile	fluxnet.ornl.gov
US-Bkg	USA	-96.8362	44.3453	AmeriFlux	(Euskirchen et al., 2017)
US-Blk	USA	-103.65	44.158	AmeriFlux	(Euskirchen et al., 2017)
US-Blo	USA	-120.633	38.8952	Fluxnet 2015	(Reichstein et al., 2003)
US-Bo1	USA	-88.2904	40.0062	LaThuile	(Stoy et al., 2013)
US-Br3	USA	-93.6936	41.9747	AmeriFlux	(Chu et al., 2018)
US-Cop	USA	-109.39	38.09	Fluxnet 2015	fluxnet.ornl.gov
US-CPk	USA	-106.119	41.068	AmeriFlux	(Chu et al., 2018)
US-Ctn	USA	-101.847	43.95	AmeriFlux	(Euskirchen et al., 2017)
US-CZ2	USA	-119.257	37.0311	AmeriFlux	(Euskirchen et al., 2017)
US-Dix	USA	-74.4346	39.9712	AmeriFlux	(Chu et al., 2018)
US-EML	USA	-149.254	63.8784	AmeriFlux	(Belshe et al., 2012)
US-FPe	USA	-105.102	48.3077	LaThuile	(Ershadi et al., 2014)
US-FR3	USA	-97.99	29.94	AmeriFlux	(Euskirchen et al., 2017)
US-Fuf	USA	-111.762	35.089	AmeriFlux	(Amiro et al., 2010)
US-GLE	USA	-106.239	41.3644	Fluxnet 2015	fluxnet.ornl.gov
US-GMF	USA	-73.2333	41.9667	AmeriFlux	(Chu et al., 2018)
US-Goo	USA	-89.8735	34.2547	Fluxnet 2015	fluxnet.ornl.gov
US-Ha1	USA	-72.1715	42.5378	LaThuile	(Barford et al., 2001)
US-Ho2	USA	-68.747	45.2091	LaThuile	(Wei et al., 2014)
US-IB2	USA	-88.241	41.8406	AmeriFlux	(Allison et al., 2005)
US-Ivo	USA	-155.75	68.4865	AmeriFlux	(Euskirchen et al., 2017)
US-Kon	USA	-96.5603	39.0824	AmeriFlux	(Antunes et al., 2001)
US-KS2	USA	-80.6715	28.60858	Fluxnet 2015	fluxnet.ornl.gov
US-KUT	USA	-93.1863	44.995	AmeriFlux	(Euskirchen et al., 2017)
US-Los	USA	-89.9792	46.0827	Fluxnet 2015	(Baker et al., 2003)
US-Me1	USA	-121.5	44.5794	Fluxnet 2015	(Irvine & Hibbard, 2007)
US-Me2	USA	-121.557	44.4523	Fluxnet 2015	(Irvine & Hibbard, 2007)
US-MMS	USA	-86.4131	39.3231	Fluxnet 2015	(Baldocchi et al., 2001)
US-MOz	USA	-92.2	38.7441	LaThuile	(Stoy et al., 2013)
US-Mpj	USA	-106.238	34.4384	AmeriFlux	(Anderson-Teixeira et al., 2011)
US-MRf	USA	-123.552	44.6465	AmeriFlux	(Chu et al., 2018)
US-Myb	USA	-121.765	38.0498	AmeriFlux	(Baldocchi et al., 2018)
US-Ne1	USA	-96.4766	41.1651	Fluxnet 2015	fluxnet.ornl.gov
US-NR1	USA	-105.546	40.0329	Fluxnet 2015	(Albert et al., 2017)
US-Oho	USA	-83.8438	41.5545	Fluxnet 2015	(Stoy et al., 2013)
US-PFa	USA	-90.2723	45.9459	LaThuile	(Keppel et al., 2012)
US-Pon	USA	-97.1333	36.7667	AmeriFlux	(Euskirchen et al., 2017)
US-Prr	USA	-147.488	65.1237	Fluxnet 2015	(Ikawa et al., 2015)

US-RC1	USA	-117.078	46.7837	AmeriFlux	(Chi et al, 2017a)
US-RC3	USA	-118.598	46.991	AmeriFlux	(Chi et al, 2017a)
US-RC4	USA	-116.949	46.758	AmeriFlux	(Chi et al, 2017a)
US-RC5	USA	-119.248	47.01	AmeriFlux	(Chi et al, 2017b)
US-Rls	USA	-116.736	43.1439	AmeriFlux	(Euskirchen et al., 2017)
US-Ro1	USA	-93.0898	44.7143	AmeriFlux	(Baker et al., 2003)
US-SCd	USA	-116.372	33.6518	AmeriFlux	(Euskirchen et al., 2017)
US-SCf	USA	-116.772	33.8079	AmeriFlux	(Euskirchen et al., 2017)
US-SCs	USA	-117.696	33.7343	AmeriFlux	(Euskirchen et al., 2017)
US-Sdh	USA	-101.407	42.0693	AmeriFlux	(Billesbach and Arkebauer, 2004)
US-Ses	USA	-106.744	34.3349	AmeriFlux	(Anderson-Teixeira et al., 2011)
US-SFP	USA	-96.902	43.2408	AmeriFlux	(Euskirchen et al., 2017)
US-Shd	USA	-96.6833	36.9333	AmeriFlux	(Burba et al., 2001)
US-Skr	USA	-81.0776	25.3629	AmeriFlux	(Barr et al., 2013)
US-Slt	USA	-74.596	39.9138	AmeriFlux	(Chu et al., 2018)
US-SP1	USA	-82.2188	29.7381	AmeriFlux	(Burton et al., 2002)
US-SP2	USA	-82.2448	29.7648	LaThuile	(Castro et al., 2000)
US-SP3	USA	-82.1633	29.7548	AmeriFlux	(Castro et al., 2000)
US-SRM	USA	-110.866	31.8214	AmeriFlux	(Barron-Gafford et al., 2013)
US-Srr	USA	-122.026	38.2006	AmeriFlux	(Chu et al., 2018)
US-SuW	USA	-156.491	20.8246	AmeriFlux	(Anderson et al., 2015)
US-Syv	USA	-89.3477	46.242	Fluxnet 2015	(Chu et al., 2018)
US-Twt	USA	-121.652	38.1055	Fluxnet 2015	(Baldocchi et al., 2018)
US-UMd	USA	-84.6975	45.5625	AmeriFlux	(Chu et al., 2018)
US-Var	USA	-120.951	38.4133	Fluxnet 2015	(Baldocchi et al., 2004)
US-WBW	USA	-84.2874	35.9588	LaThuile	(Baldocchi et al., 2004)
US-WCr	USA	-90.0799	45.8059	Fluxnet 2015	(Baker et al., 2003)
US-Wdn	USA	-106.262	40.7838	AmeriFlux	(Euskirchen et al., 2017)
US-Whs	USA	-110.052	31.7438	AmeriFlux	(Biederman, et al., 2016)
US-Wi4	USA	-91.1663	46.7393	LaThuile	(Hilton et al., 2014)
US-Wi6	USA	-91.2982	46.6249	Fluxnet 2015	(Noormets et al., 2007)
US-Wjs	USA	-105.862	34.4255	AmeriFlux	(Anderson-Teixeira et al., 2011)
US-Wkg	USA	-109.942	31.7365	Fluxnet 2015	(Biederman, et al., 2016)
US-Wrc	USA	-121.952	45.8205	AmeriFlux	(Chu et al., 2018)
RU-YLF	Russia	129.2414	62.255	AsiaFlux	asiaflux.net
RU-YPF	Russia	129.6506	62.24139	AsiaFlux	asiaflux.net
ZA-Kru	South Africa	31.4969	-25.0197	LaThuile	(King et al., 2003)
ZM-Mon	Zambia	23.25278	-15.4378	Fluxnet 2015	(King et al., 2003)

20

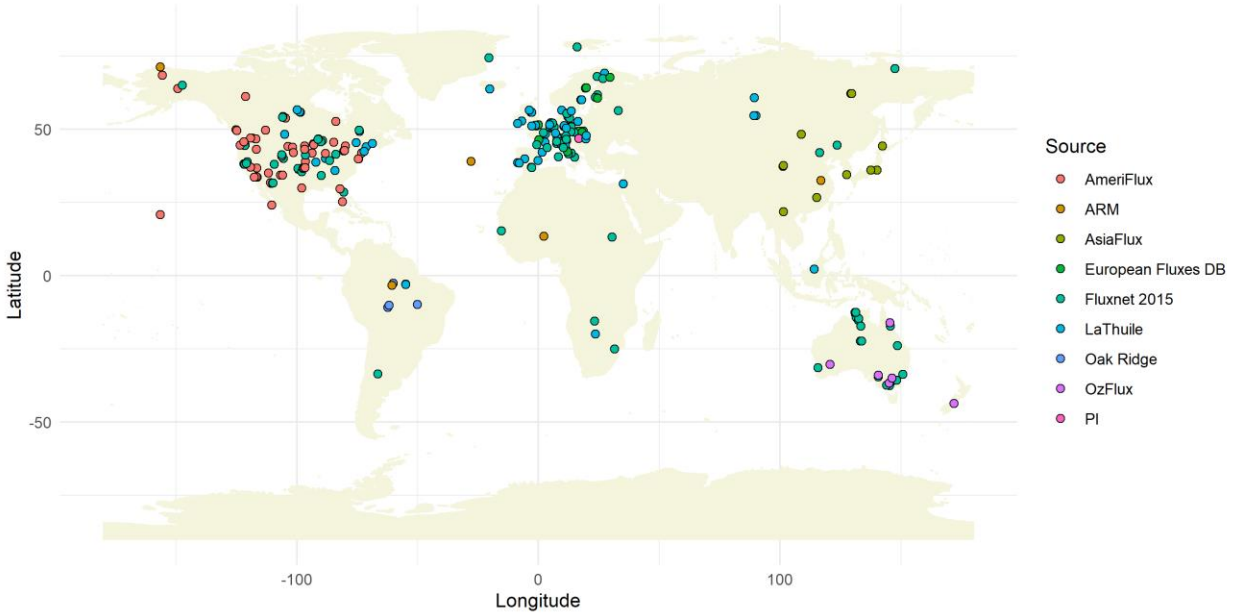

Figure S1: Location of the 260 sites used to derive and validate DOLCE V2, color-coded by data source. Data source includes Ameriflux (ameriflux.lbl.gov), the Atmospheric Radiation Measurement (ARM; arm.gov), AsiaFlux (asiaflux.net), European Fluxes Database (europe-fluxdata.eu), Fluxnet 2015, LaThuile Free Fair Use (fluxnet.fluxdata.org), Oak Ridge data repository (daac.ornl.gov), OzFlux (ozflux.org.au) and individual site principal investigators (PI).

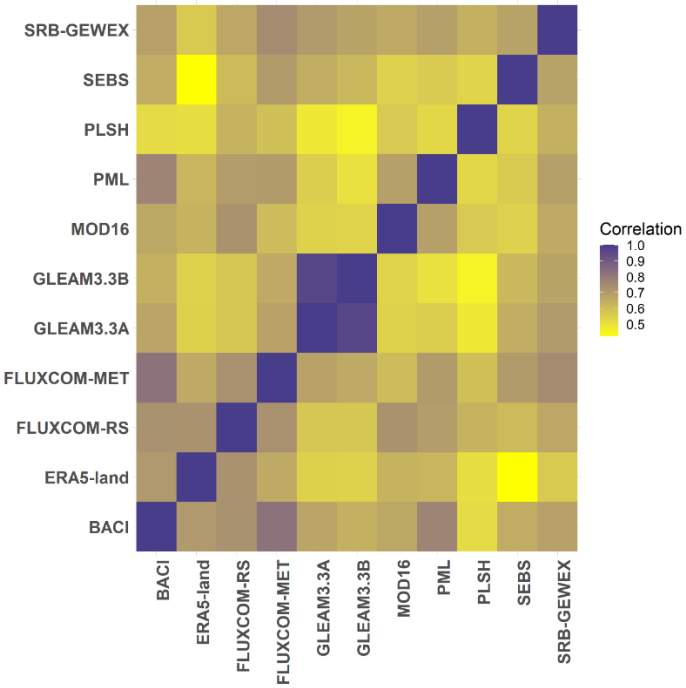

Figure S2: Error correlation between the participating parent datasets of DOLCE V2 when compared to in-situ data from 260 sites. Large correlation (>0.5) between two datasets indicates that their errors are highly dependent.

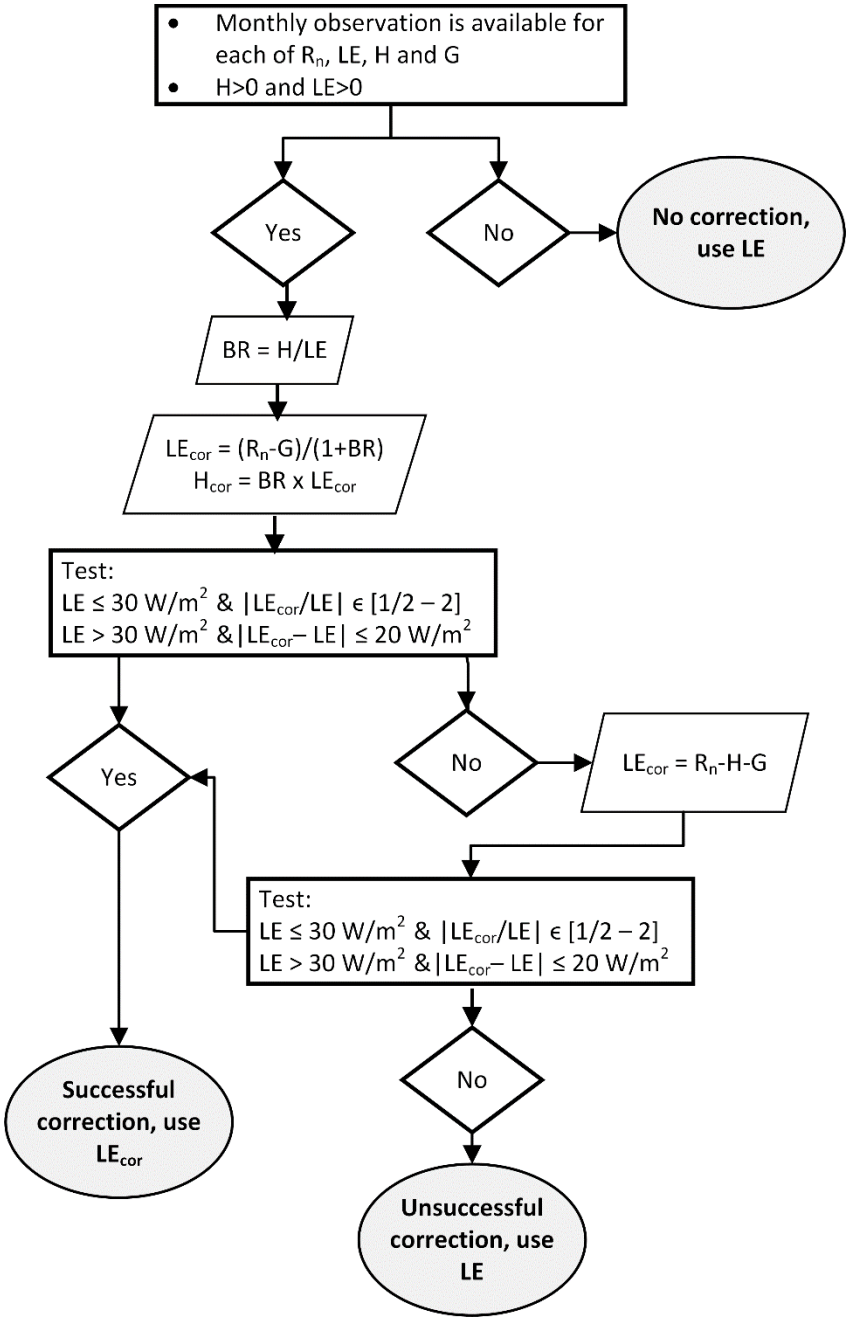

Figure S3: Flowchart illustrating the correction steps carried out for every monthly record of observed LE at the flux tower sites to correct for energy balance non-closure.

S2. Global ET datasets

Table S2: Access information and download data of the global ET datasets (also referred to as parent datasets) used to develop DOLCE V2 and DOLCE V3.

Dataset	Access to data	Download date

BACI	https://doi.org/10.17871/BACI.224	03-10-2019
ERA5-land	https://doi.org/10.24381/cds.e2161bac	05-06-2020
FLUXCOM-RS	https://doi.org/10.17871/FLUXCOM_EnergyFluxes_v1 LE.RS.EBC-BWR.MLM-ANN.METEO-NONE.4320_2160.monthly	02-10-2019
FLUXCOM-MET or FLUXCOM-METa	https://doi.org/10.17871/FLUXCOM_EnergyFluxes_v1 LE.RS_METEO.EBC-BWR.MLM-MARS.METEO-GSWP3.720_360.monthly	02-10-2019
FLUXCOM-MET FLUXCOM-METb	https://doi.org/10.17871/FLUXCOM_EnergyFluxes_v1 LE.RS_METEO.EBC-ALL.MLM-ALL.METEO-CRUNCEP_v8.720_360.monthly	15-03-2021
GLEAM3.3A	www.GLEAM.eu	02-09-2019
GLEAM3.3B	www.GLEAM.eu	02-09-2019
GLEAM3.5A	www.GLEAM.eu	18-03-2021
GLEAM3.5B	www.GLEAM.eu	18-03-2021
MOD16	http://files.ntsg.umt.edu/data/NTSG_Products/MOD16/ MOD16A2_MONTHLY.MERRA_GMAO_1kmALB/GEOTIFF_0.05degree/	01-10-2019
PML	https://data.csiro.au/collections/#collection/CIcsiro:17375v2	09-04-2019
PLSH	http://files.ntsg.umt.edu/data/ET_global_monthly/Global_8kmResolution/	30-09-2019
SEBS	http://en.tpedatabase.cn/portal/MetaDataInfo.jsp?MetaDataId=249454	09-04-2019
SRB-GEWEX	https://disc.gsfc.nasa.gov/datasets/WC_PM_ET_050_1/summary	01-10-2019

S3. Weighting groups

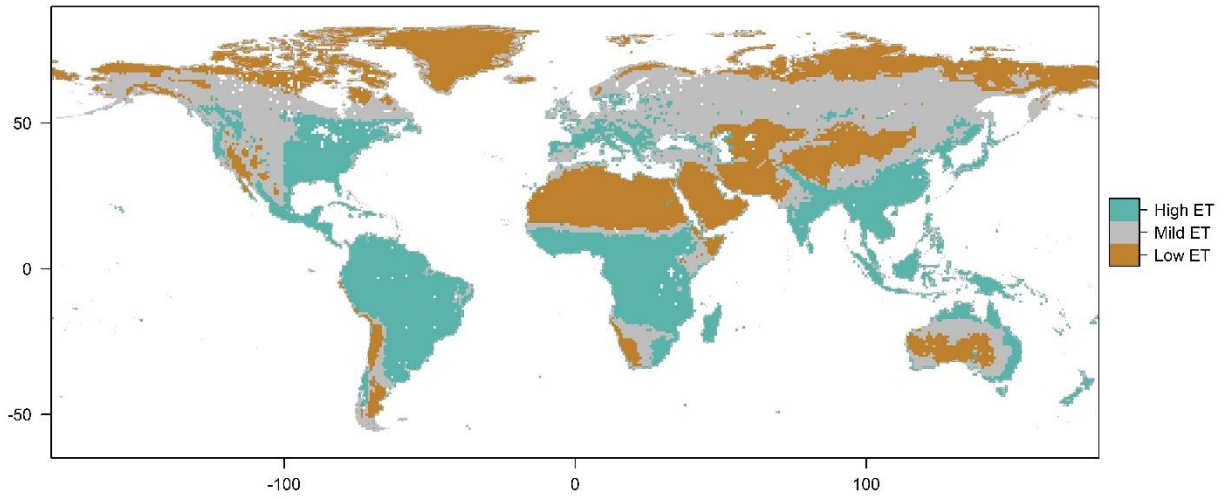

Figure S4: Classification of the land into three distinct broad ET regimes according to two aspects of ET, mean annual total ET and within-year relative variability throughout 1980 – 2018, derived from GLEAM V3.5a, and using K-means unsupervised classification.

S4. Bias correction strategies

In DOLCE V1, we showed that part of the success of the weighting approach is due to the bias correction applied before the weighting. Within each tier, the bias correction is applied simply by adding the mean difference between a product and tower data uniformly to all values of a product before the weights are derived – it is constant in space and time for a given product within one tier. The grouping strategies detailed above examine the effect of considering different bias correction and weighting subgroups

within each spatiotemporal tier, with groups divided by region (continents, latitudes, or ET regimes) or/and seasons. As an alternative to the grouping strategies, we also investigate if deriving a spatially varying bias correction within each tier could further improve the weighting. A spatially varying bias correction might better capture the performance deficiencies of each the parent datasets.

To derive a global bias correction for a particular parent dataset within each tier, we first compute the mean bias at each flux tower site across all the time records within the tier. We then assign those ET bias values, or bias field, to the grid cells containing the sites. Finally, using the bias values at these grid cells, we extrapolate the bias field spatially to the entire global land domain within the tier using several different extrapolation strategies, including inverse distance weighting (IDW), local polynomial interpolation and nearest neighbourhood. As with the different weighting groups, we test the effectiveness of each approach using out-of-sample tests. The hybrid ET estimates derived by implementing spatially varying bias correction strategies failed to outperform the parent datasets in the out-of-sample site tests. Figure S5 shows the results of out-of-sample tests for the bias correction approach that uses IDW.

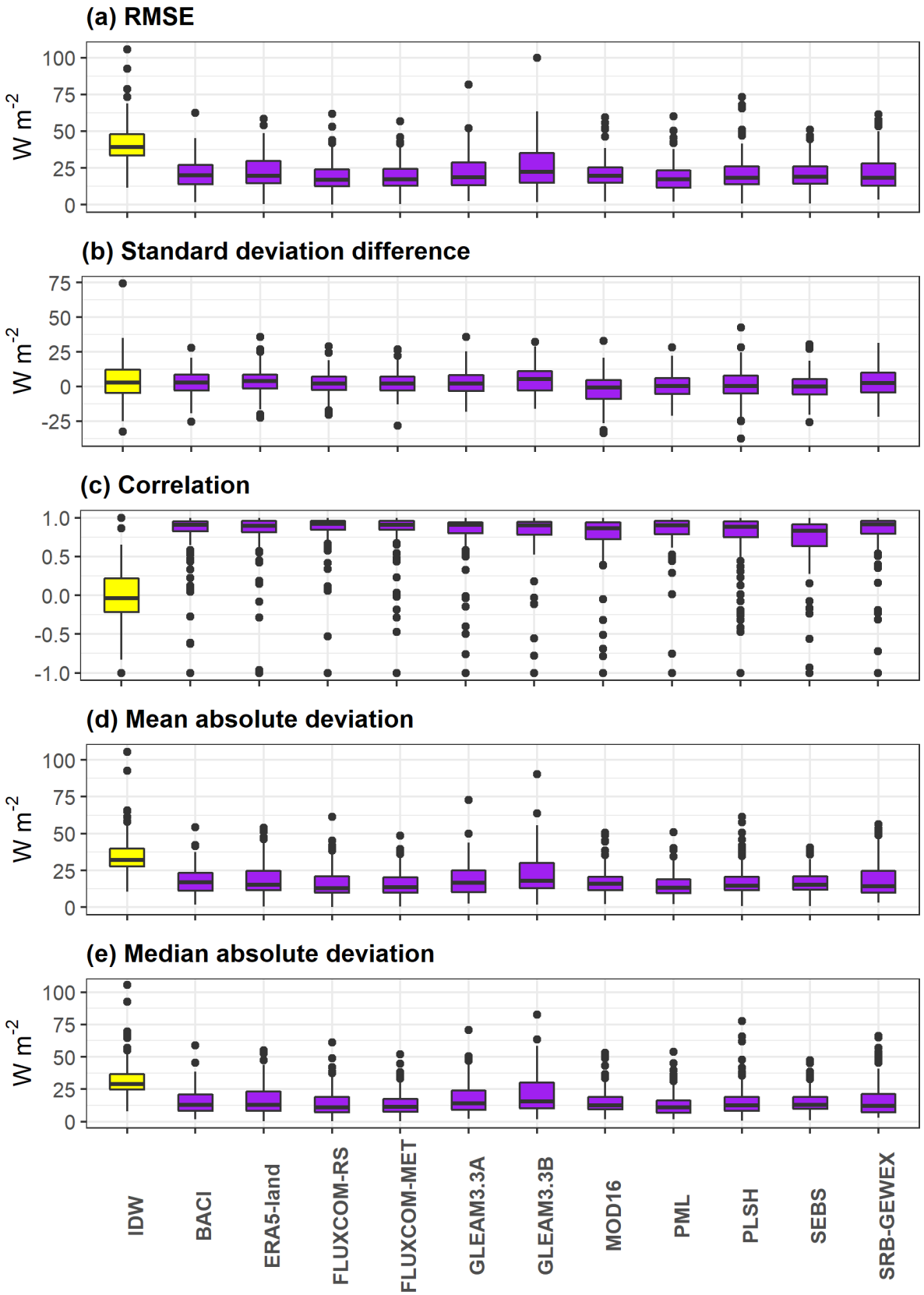
(a) RMSE
W m-2
100
75
50
25
0
(b) Standard deviation difference
W m-2
75
50
25
0
-25
(c) Correlation
1.0
0.5
0.0
-0.5
-1.0
(d) Mean absolute deviation
W m-2
100
75
50
25
0
(e) Median absolute deviation
W m-2
100
75
50
25
0
IDW
BACI
ERA5-land
FLUXCOM-RS
FLUXCOM-MET
GLEAM3.3A
GLEAM3.3B
MOD16
PML
PLSH
SEBS
SRB-GEWEX

72

Figure S5: Results of the out-of-sample test across five metrics of performance, (a) RMSE, (b) Correlation (c) Standard deviation difference , (d) Mean absolute deviation , and (e) Median absolute deviation. Box plots represent spread over 1000 different selections of out-of-sample sites. The yellow box plot represents the performance results of weighting using IDW bias correction strategy, while the purple boxplots represent performance results of the parent datasets.

S5. Performance of weighting group strategies

The results of out-of-sample performance of different grouping strategies (including no grouping) against the 11 parent datasets of DOLCE V2 (left column) are presented in Fig. S6. The performance results across all 1000 different random site samples are shown in a boxplot for each clustering method (yellow), non-clustered weighting (as per DOLCE V1, in magenta, labelled NO.GROUPING), and each parent dataset (purple). The hybrid ET estimates derived from grouped weighting are labelled LAT.ZONES, CONTINENTS, SEASONS, MONTHS, and HEMISPHERE, following the grouping approaches outlined above. The plots in the left column show that overall, the hybrid ET estimates outperform their 11 parent datasets across all the performance metrics and in all clustering settings. To highlight the differences between the grouping strategies, we magnify the leftmost section of these plots in the right column of Fig. S6, and we also show in red the median value of each boxplot. Results only change slightly across the grouping approaches, with the best results achieved by grouping weights by months. Despite the relatively small improvement offered by this strategy at the out-of-sample sites over the other grouping strategies, we derive DOLCE V2 (Hobeichi, 2020) by applying a grouped weighting by months. We recall that in this approach, the observational and gridded ET data are split into two groups, one covering the period June – November and the other covering December – May. Weighting and bias correction is then implemented in each group separately for each tier to create the subsets from which the hybrid ET product is derived.

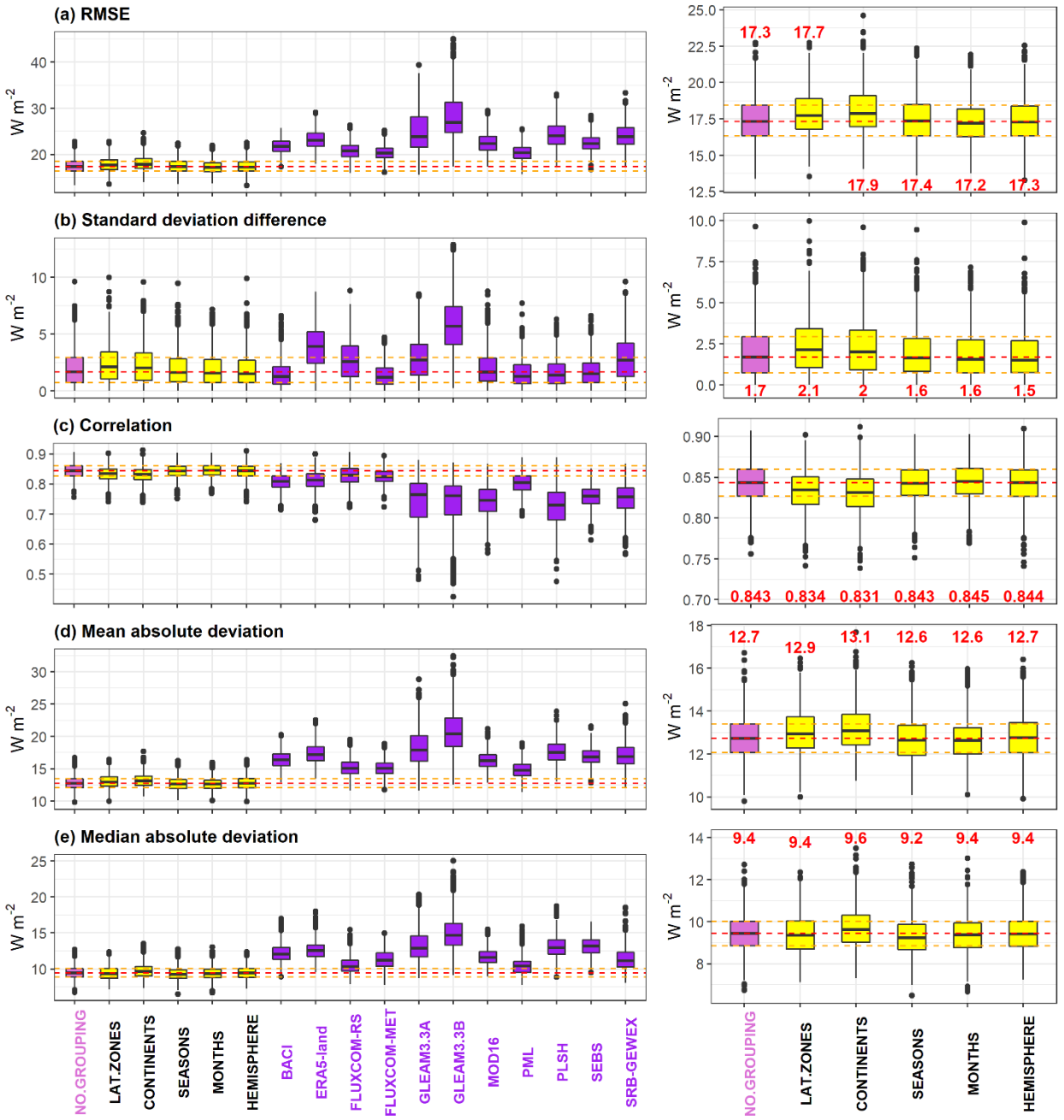

Figure S6: Results of the out-of-sample test across five metrics of performance, (a) RMSE, (b) Correlation (c) Standard deviation difference , (d) Mean absolute deviation , and (e) Median absolute deviation. Box plots represent spread over 1000 different selections of out-of-sample sites. Different clustering methods (yellow) include: no clustering (NO.GROUPING; shown in magenta and horizontal dashed lines), by latitude (LATZONES), by continents (CONTINENTS), by seasons (SEASONS), by months (MONTHS), and by hemisphere (HEMISPHERE), the red text marks the median values. Performance comparison with each of the parent datasets is shown in purple.

The box plots in Fig. S7 show the ratio $\frac{\text{Uncertainty}_{\text{in-sample}}}{\text{Uncertainty}_{\text{out-sample}}}$, obtained across the different grouping techniques. Each boxplot represents this ratio from all sites out of sample and shows that over half of the data, the ratio ranges between 0.83 and 1.51, with a median very close to 1. This confirms that, overall, when the uncertainty estimates are computed out of sample, they are very similar to what they would have been if they were computed in sample. Also, the fact the shift in ratio is mostly towards values bigger than 1 rather than smaller than 1 indicates that $\text{Uncertainty}_{\text{in-sample}}$ is greater than $\text{Uncertainty}_{\text{out-sample}}$ so that uncertainty is overestimated rather than underestimated. Interestingly, the lower (0.86) and upper (1.46) quartiles achieved by grouping weighting by months are the closest to 1 than the other grouping techniques. This suggests that overall, grouping weighting by months is able to derive slightly more robust uncertainty estimates than the other techniques.

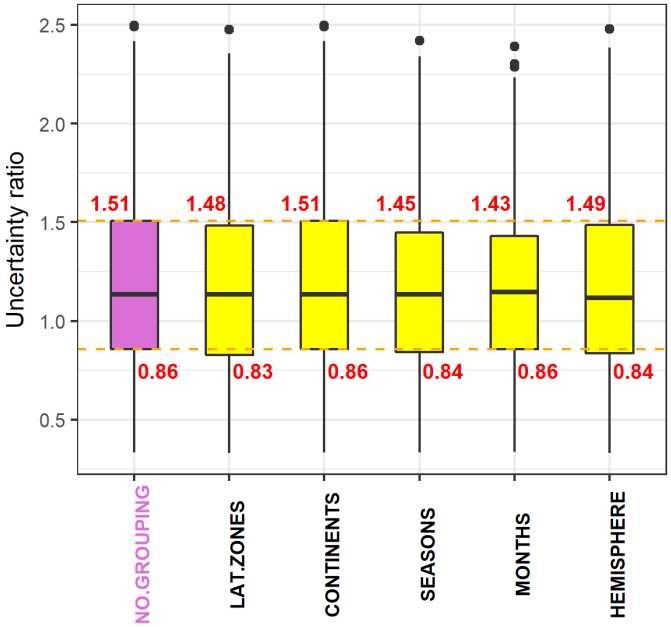

Figure S7: Box and whisker plots displaying the ratio $\frac{Uncertainty_{in-sample}}{Uncertainty_{out-sample}}$, computed for each site using the clustering methods defined in Sect. 2.2.4. Labeling and colors are as in Fig. S6. Red text marks the value of the upper quantile (75%) and lower quantile (25%).

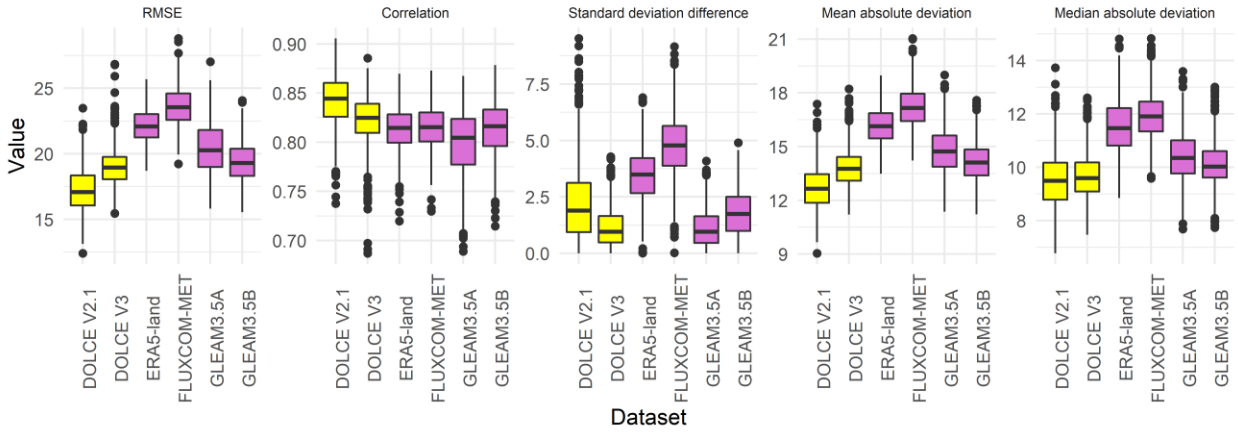

Figure S8: Results of the out-of-sample test comparing DOLCE V3 with DOLCE V2.1 (both in yellow) and each of its parent datasets (purple) across five metrics of performance, RMSE, Correlation, Standard deviation difference , Mean absolute deviation , and Median absolute deviation. Box plots represent spread over 1000 different selections of out-of-sample sites.

S6. Comparison of DOLCE V3 with its parent datasets

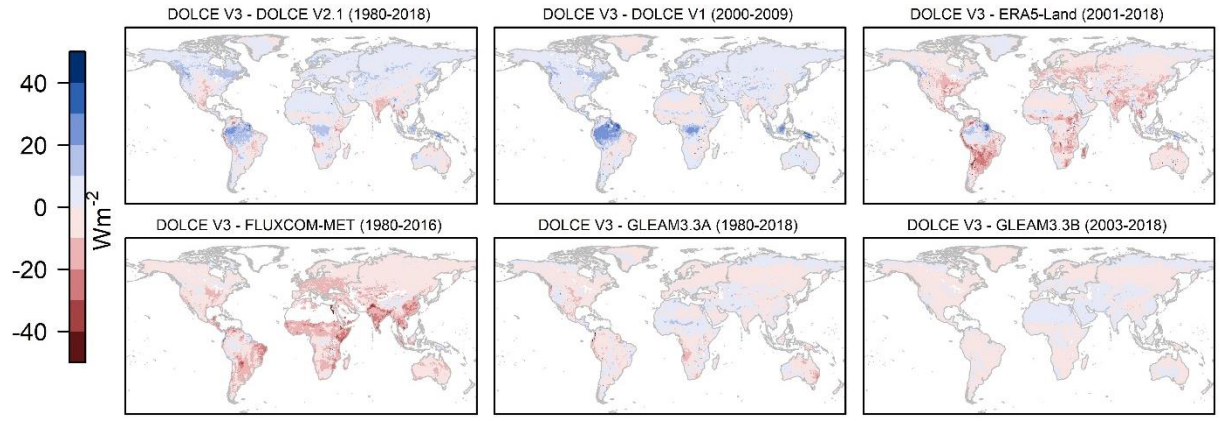

Figure S9: Spatial distribution of differences in ET climatology between DOLCE V3 and each of its parent datasets and DOLCE V2. Different spatiotemporal masks are applied for each comparison based on the spatiotemporal coverage of DOLCE V3 and the other datasets.

S7. Performance of DOLCE V2 at flux sites

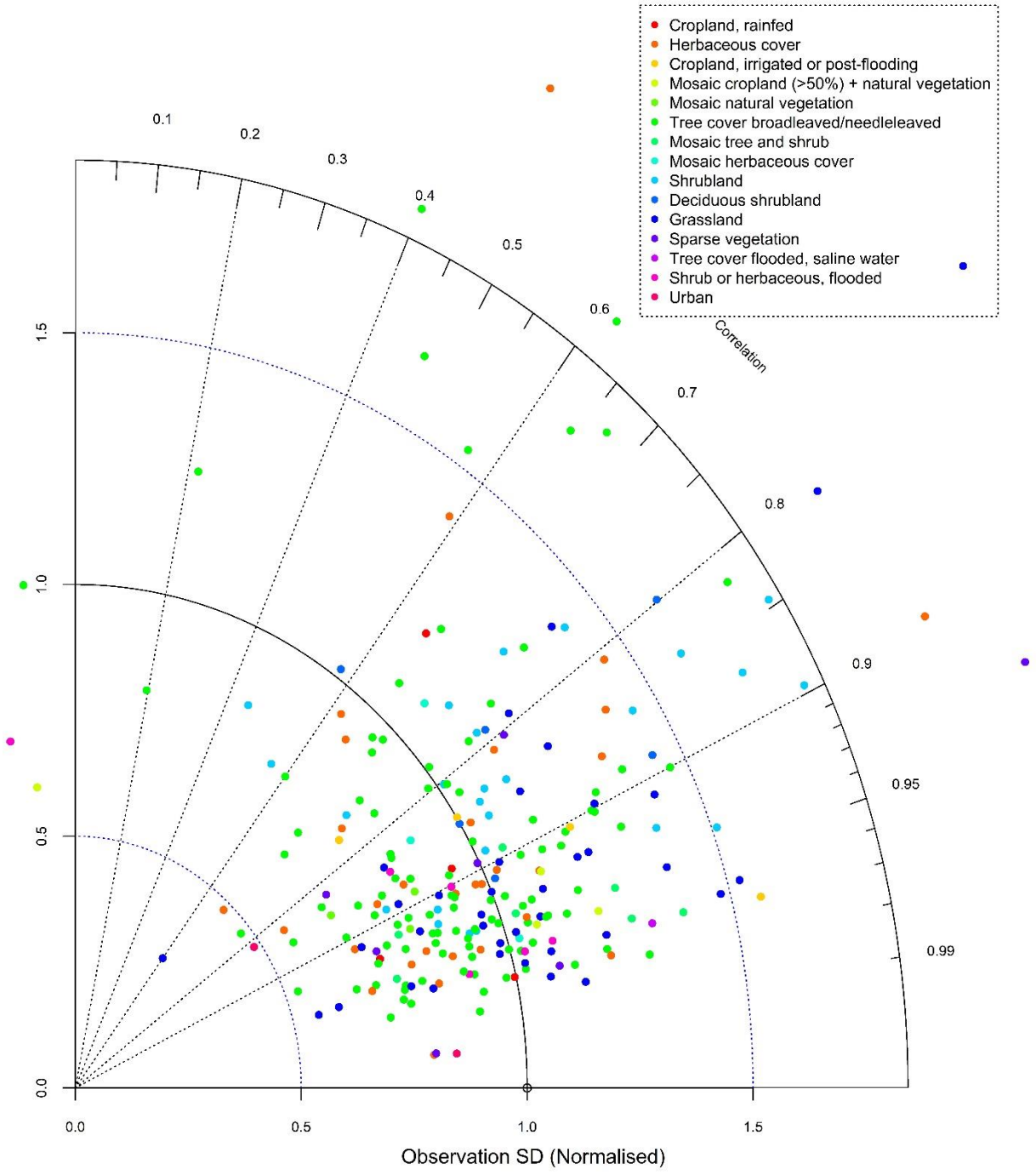

Figure S10: Taylor Diagram displaying two statistical metrics i.e., correlation and standard deviation of DOLCE V2 relative to normalised observational data presented by a hollow point (reference point) at one unit on the x-axis. Statistics points are color-coded by the land cover of the sites they represent. Land covers at the site locations are based on land cover maps from the European Space Agency (ESA;

http://www.esa.int/). All broadleaved and needleleaved tree covers were combined together in a single land cover 'Tree cover broadleaved/needleleaved'.

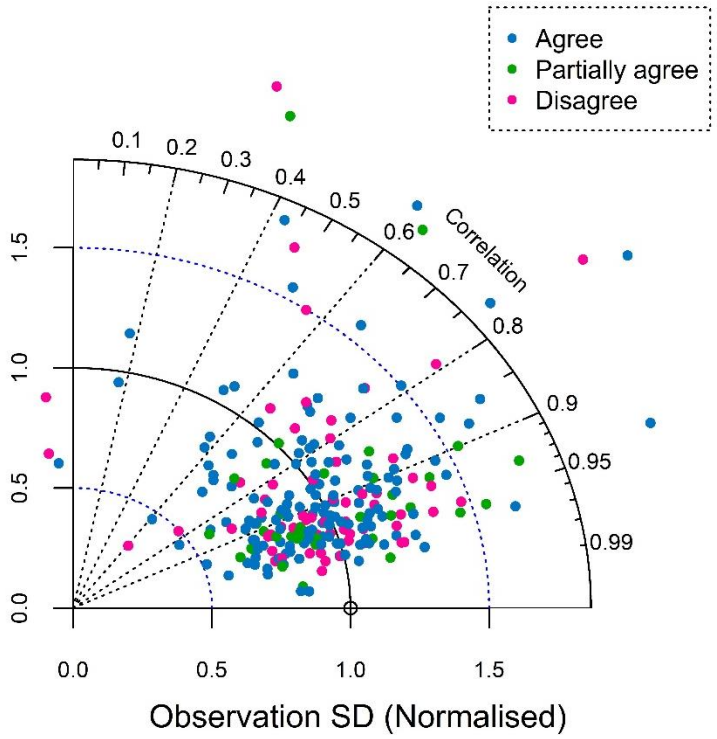

Figure S11: Taylor Diagram displaying two statistical metrics i.e., correlation and standard deviation of DOLCE V2 relative to normalised observational data presented by a hollow point (reference point) at one unit on the x-axis. Blue points represent sites whose land types match the dominant land types of the underlying grid-cells; green points represent sites whose land types cover more than 25% of the underlying grid-cells without being the dominant land cover at these grid-cells; and pink points representing sites whose land types covers less than 25% of the underlying grid-cells. Land cover types at the sites' footprint and the underlying grid-cells are determined based on land cover maps from the European Space Agency.

S8. Comparison of DOLCE V2 with DOLCE V1 and Conserving Land Atmosphere Synthesis Suite (CLASS-ET)

Table S3: Area weighted mean ET (Wm^{-2}) computed for DOLCE V2, DOLCE V1 and CLASS-ET and averaged over each of Africa, Australia, Eurasia, North America, South America and the global land excluding Antractica. The differences between DOLCE V2 and each of DOLCE V1 and CLASS-ET are shown in columns 5 and 6 respectively.

	DOLCE V2	DOLCE V1	CLASS	DOLCE V2 – DOLCE V1	DOLCE V2 – CLASS
Africa	40.1	35.8	36.3	4.3	3.8

Australia	25.4	23	26.1	2.4	-0.7
Eurasia	29.3	28	27.7	1.3	1.6
North America	33.2	30.5	31.1	2.7	2.1
South America	73.3	68.3	71.2	5	2.1
Global land excluding Antarctica	38.4	35.7	36.3	2.7	2.1

S9. ET regimes

Table S4: List of 6 ET regimes identified by unsupervised learning. Second column shows the abbreviation given to each regime. Third and fourth columns display the statistics of the class's centroid: Yearly ET total climatology (column 3) and relative within-year standard deviation of monthly ET climatology (column 4).

Regime description	Regime abbreviation	Yearly ET total climatology (mm)	Relative standard deviation (%)
Very low ET with high variability	V.L.ET, H.variability	60	10.5
Low ET with high variability	L.ET, H.variability	250.8	8.7
Mild low ET with medium variability	M.L.ET, M.variability	435.4	7.2
Mild high ET with medium variability	M.H.ET, M.variability	680.3	4.7
High ET with low variability	H.ET, L.variability	973.7	2.7
Very high ET with low variability	V.H.ET, L.variability	1408.2	0.9

S10. References

Albert, L. P., Keenan, T. F., Burns, S. P., Huxman, T. E., and Monson, R. K.: Climate Controls Over Ecosystem Metabolism: Insights From A Fifteen-Year Inductive Artificial Neural Network Synthesis For A Subalpine Forest, Oecologia, 184(1), 25-41, 2017.

Allison, V. J., Miller, R. M., Jastrow, J. D., Matamala, R., Zak, D. R.: Changes In Soil Microbial Community Structure In A Tallgrass Prairie Chronosequence, Soil Science Society Of America Journal, 69(5), 1412-1421, 2005.

Amiro, B. D., Barr, A. G., Barr, J. G., Black, T. A., Bracho, R., Brown, M., Chen, J., Clark, K. L., Davis, K. J., Desai, A. R., Dore, S., Engel, V., Fuentes, J. D., Goldstein, A. H., Goulden, M. L., Kolb, T. E., Lavigne, M. B., Law, B. E., Margolis, H. A., Martin, T.,

McCaughey, J. H., Misson, L., Montes-Helu, M., Noormets, A., Randerson, J. T., Starr, and G., Xiao, J.: (2010) Ecosystem Carbon Dioxide Fluxes After Disturbance In Forests Of North America, J. Geophys. Res. Atmos., 115(G00K02).
Anderson, R. G., Tirado-Corbalá, R., Wang, D., and Ayars, J. E.: Long-Rotation Sugarcane In Hawaii Sustains High Carbon Accumulation And Radiation Use Efficiency In 2nd Year Of Growth, Agriculture, Ecosystems & Environment, 199, 216-224, 2015.
Anderson-Teixeira, K. J., Delong, J. P., Fox, A. M., Brese, D. A., and Litvak, M. E.: Differential Responses Of Production And Respiration To Temperature And Moisture Drive The Carbon Balance Across A Climatic Gradient In New Mexico, Glob. Chang. Biol., 17(1), 410-424, 2011.
Andrykanus, R.: Howard Springs Understory_old_20131128 OzFlux: Australian and New Zealand Flux Research and Monitoring hdl: 102.100.100/14224, 2012.
Antunes, M. A. H., Walter-Shea, E. A., and Mesarch, M. A.: Test Of An Extended Mathematical Approach To Calculate Maize Leaf Area Index And Leaf Angle Distribution, Agric. For. Meteorol., 108(1), 45-53, 2001.
Arain, M. A. and Restrepo-Coupe, N.: Net Ecosystem Production In A Temperate Pine Plantation In Southeastern Canada, Agric. For. Meteorol., 128(3-4), 223-241, 2005.
Bagley, J. E., Kueppers, L. M., Billesbach, D. P., Williams, I. N., Biraud, S. C., and Torn, M. S.: The Influence Of Land Cover On Surface Energy Partitioning And Evaporative Fraction Regimes In The U.S. Southern Great Plains, J. Geophys. Res. Atmos.: Atmospheres, 122(11), 5793-5807, 2017.
Atmospheric Radiation Measurement (ARM) user facility, updated hourly. Eddy Correlation Flux Measurement System (30ECOR). 1997-04-25 to 2004-03-31, Southern Great Plains (SGP) Smileyberg, KS (ABLE) (A4). Compiled by R. Sullivan, M. Pekour and E. Keeler. ARM Data Center. Data set accessed 2019-09-17 at doi:10.5439/1025039, 1997.
Atmospheric Radiation Measurement (ARM) user facility updated hourly. Quality Controlled Eddy Correlation Flux Measurement (30QCECOR). 2005-11-26 to 2007-01-07, ARM Mobile Facility (NIM) Niamey, Niger (M1). Compiled by R. McCoy, S. Xie and Y. Zhang. ARM Data Center. Data set accessed 2019-09-17 at doi:10.5439/1097546, 2005.
Atmospheric Radiation Measurement (ARM) user facility, updated hourly. Quality Controlled Eddy Correlation Flux Measurement (30QCECOR). 2008-05-06 to 2008-12-28, ARM Mobile Facility (HFE) Shouxian, Anhui, China (M1). Compiled by R. McCoy, S. Xie and Y. Zhang. ARM Data Center. Data set accessed 2019-09-17 at doi:10.5439/1097546, 2008.
Atmospheric Radiation Measurement (ARM) user facility, updated hourly. Quality Controlled Eddy Correlation Flux Measurement (30QCECOR). 2009-04-15 to 2010-09-30, ARM Mobile Facility (GRW) Graciosa Island, Azores, Portugal; AMF1 (M1). Compiled by R. McCoy, S. Xie and Y. Zhang. ARM Data Center. Data set accessed 2019-09-17 at doi:10.5439/1097546, 2009.
Atmospheric Radiation Measurement (ARM) user facility, updated hourly. Quality Controlled Eddy Correlation Flux Measurement (30QCECOR). 2011-09-16 to 2020-05-11, North Slope Alaska (NSA) Barrow, Alaska (71.325, -156.608, 5) (E10). Compiled by R. McCoy, S. Xie and Y. Zhang. ARM Data Center. Data set accessed 2019-09-17 at doi:10.5439/1097546, 2011.
Atmospheric Radiation Measurement (ARM) user facility, updated hourly. Eddy Correlation Flux Measurement System (30ECOR). 2013-12-05 to 2015-01-10, Tropical Western Pacific (TWP) East Arm, Darwin, Australia (E30). Compiled by R. Sullivan, D. Cook and E. Keeler. ARM Data Center. Data set accessed 2019-09-17 at doi:10.5439/1025039, 2013.
Aurela, M., Laurila, T. and Tuovinen, J.-P.: Seasonal CO2 balances of a subarctic mire, J. Geophys. Res. Atmos., 106(D2), 1623–1637, doi:10.1029/2000JD900481, 2001.
Baker, I., Denning, A. S., Hanan, N., Prihodko, L., Uliasz, M., Vidale, P., Davis, and K., Bakwin, P.: Simulated And Observed Fluxes Of Sensible And Latent Heat And CO2 At The WLEF-TV Tower Using SiB2.5, Glob. Chang. Biol., 9(9), 1262-1277, 2003.
Baldocchi, D. D., Law, B. E., and Anthoni, P. M.: On Measuring And Modeling Energy Fluxes Above The Floor Of A Homogeneous And Heterogeneous Conifer Forest, Agric. For. Meteorol., 102(2-3), 187-206, 2000.
Baldocchi, D., Falge, E., Gu, L., Olson, R., Hollinger, D., Running, S., Anthoni, P., Bernhofer, C., Davis, K., Evans, R., Fuentes, J., Goldstein, A., Katul, G., Law, B., Lee, X., Malhi, Y., Meyers, T., Munger, W., Oechel, W., Paw, K. T., Pilegaard, K., Schmid, H. P., Valentini, R., Verma, S., Vesala, T., Wilson, K. and Wofsy, S.: FLUXNET: A New Tool to Study the Temporal and Spatial Variability of Ecosystem–Scale Carbon Dioxide, Water Vapor, and Energy Flux Densities, Bull. Am. Meteorol. Soc., 82(11), 2415–2434, doi:10.1175/1520-0477(2001)082<2415:FANTTS>2.3.CO;2, 2001.
Baldocchi, D. D., Xu, L., and Kiang, N.: How Plant Functional-Type, Weather, Seasonal Drought, And Soil Physical Properties Alter Water And Energy Fluxes Of An Oak–Grass Savanna And An Annual Grassland, Agric. For. Meteorol., 123(1-2), 13-39, 2004.
Baldocchi, D. and Sturtevant, C.: Does day and night sampling reduce spurious correlation between canopy photosynthesis and ecosystem respiration?, Agric. For. Meteorol., 207(), 117-126, 2015.
Baldocchi, D., Penuelas, J.: The Physics And Ecology Of Mining Carbon Dioxide From The Atmosphere By Ecosystems, Glob. Chang. Biol., 256-257(2), 179-195, 2018.
Barcza, Z., Kern, A., Haszpra, L. and Kljun, N.: Spatial representativeness of tall tower eddy covariance measurements using

remote sensing and footprint analysis, Agric. For. Meteorol., 149(5), 795–807, doi:10.1016/j.agrformet.2008.10.021, 2009.
Barford, C. C., Wofsy, S. C., Goulden, M. L., Munger, J. W., Pyle, E. H., Urbanski, S. P., Hutyra, L., Saleska, S. R., Fitzjarrald, D., and Moore, K.: Factors Controlling Long- And Short-Term Sequestration Of Atmospheric CO2 In A Mid-Latitude Forest, Science, 294(5547), 1688-1691, 2001.
Barr, A. G., Griffis, T. J., Black, T. A., Lee, X., Staebler, R. M., Fuentes, J. D., Chen, Z., Morgenstern, K.: Comparing The Carbon Budgets Of Boreal And Temperate Deciduous Forest Stands, Canadian Journal Of Forest Research, 32(5), 813-822, 2002.
Barr, J. G., Engel, V., Fuentes, J. D., Fuller, D. O., Kwon, H.: Modeling Light Use Efficiency In A Subtropical Mangrove Forest Equipped With Co2 Eddy Covariance, Biogeosciences, 10(3), 2145-2158, 2013.
Barron-Gafford, G. A., Scott, R. L., Jenerette, G. D., Hamerlynck, E. P., Huxman, T. E. (2013) Landscape And Environmental Controls Over Leaf And Ecosystem Carbon Dioxide Fluxes Under Woody Plant Expansion, Journal Of Ecology, 101(6), 1471-1483
Belshe, E. F., Schuur, E. A., Bolker, B. M., and Bracho, R.: Incorporating Spatial Heterogeneity Created By Permafrost Thaw Into A Landscape Carbon Estimate, J. Geophys. Res. Atmos.: Biogeosciences, 117(G1), 2012.
Belelli Marchesini, L., Papale, D., Reichstein, M., Vuichard, N., Tchebakova, N. and Valentini, R.: Carbon balance assessment of a natural steppe of southern Siberia by multiple constraint approach, Biogeosciences, 4(4), 581–595, doi:10.5194/bg-4-581-2007, 2007.
Bell, T. W., Menzer, O., Troyo-Diéquez, E., Oechel, W. C.: Carbon Dioxide Exchange Over Multiple Temporal Scales In An Arid Shrub Ecosystem Near La Paz, Baja California Sur, Mexico, Glob. Chang. Biol., 18(8), 2570-2582, 2012.
Beringer, J.: Adelaide River OzFlux tower site OzFlux: Australian and New Zealand Flux Research and Monitoring hdl: 102.100.100/14228, 2013a.
Beringer, J.: Dry River OzFlux tower site OzFlux, Australian and New Zealand Flux Research and Monitoring hdl: 102.100.100/14229, 2013b.
Beringer, J.: Fogg Dam OzFlux tower site OzFlux, Australian and New Zealand Flux Research and Monitoring hdl: 102.100.100/14233, 2013c.
Beringer, J.: Sturt Plains OzFlux tower site OzFlux, Australian and New Zealand Flux Research and Monitoring hdl: 102.100.100/14230, 2013d.
Beringer, J.: Yanco JAXA OzFlux tower site OzFlux, Australian and New Zealand Flux Research and Monitoring hdl: 102.100.100/14235, 2013e.
Beringer, J.: Wallaby Creek OzFlux tower site OzFlux, Australian and New Zealand Flux Research and Monitoring hdl: 102.100.100/14231, 2013f.
Beringer, J.: Red Dirt Melon Farm OzFlux tower site OzFlux: Australian and New Zealand Flux Research and Monitoring hdl: 102.100.100/14245, 2014a.
Beringer, J., :Riggs Creek OzFlux tower site OzFlux, Australian and New Zealand Flux Research and Monitoring hdl: 102.100.100/14246, 2014b.
Beringer, J.: Whroo OzFlux site OzFlux, Australian and New Zealand Flux Research and Monitoring hdl: 102.100.100/52559, 2017.
Biederman, J. A., Scott, R. L., Goulden, M. L., Vargas, R., Litvak, M. E., Kolb, T. E., Yepez, E. A., Oechel, W. C., Blanken, P. D., Bell, T. W., Garatuza-Payan, J., Maurer, G. E., Dore, S., and Burns, S. P.: Terrestrial Carbon Balance In A Drier World: The Effects Of Water Availability In Southwestern North America, Glob. Chang. Biol., 22(5), 1867-1879, 2016.
Billesbach, D. and Arkebauer, T. J. : AmeriFlux US-SdH Nebraska SandHills Dry Valley, Dataset, doi:10.17190/AMF/1246136, 2004.
Bodesheim, J.: BACI v1, Upscaled diurnal cycles of carbon and energy fluxes. Max Planck Institute for Biogeochemistry, Jena, (accessed on 3 October 2019), https://doi.org/10.17871/BACI.224, 2017.
Burba, G. G. and Verma, S. B.: Prairie Growth, PAR Albedo And Seasonal Distribution Of Energy Fluxes, Agric. For. Meteorol., 107(3), 227-240, 2001.
Burton, A. J. and Pregitzer, K. S.: Measurement Carbon Dioxide Concentration Does Not Affect Root Respiration Of Nine Tree Species In The Field, Tree Physiology, 22(1), 67-72, 2002.
Calperum Tech; Calperum Chowilla OzFlux tower site OzFlux: Australian and New Zealand Flux Research and Monitoring hdl: 102.100.100/14236, 2013.
Campbell, J. L., Sun, O. J., and Law, B. E.: Disturbance And Net Ecosystem Production Across Three Climatically Distinct Forest Landscapes, Global Biogeochem. Cycles, 18(4), 2004.
Castro, M. S., Gholz, H. L., Clark, K. L., Steudler, P. A.: Effects Of Forest Harvesting On Soil Methane Fluxes In Florida Slash Pine Plantations, Canadian Journal Of Forest Research, 30(10), 1534-1542, 2000.
Cescatti, A. and Zorer, R.: Structural acclimation and radiation regime of silver fir (Abies alba Mill.) shoots along a light gradient, Plant, Cell Environ., 26(3), 429–442, doi:10.1046/j.1365-3040.2003.00974.x, 2003.

Chen, J. M., Govind, A., Sonnentag, O., Zhang, Y., Barr, and A., Amiro, B.: Leaf Area Index Measurements At Fluxnet-Canada Forest Sites, Agric. For. Meteorol., 140(1-4), 257-268, 2006.
Chen, X.: Surface energy balance based global land evapotranspiration (SEBS) Daily ET dataset: (accessed on 9 April 2019), http://en.tpedatabase.cn/portal/MetaDataInfo.jsp?MetaDataId=249454, 2017.
Chi, J., Maureira, F., Waldo, S., Pressley, S. N., Stöckle, C. O., O'Keeffe, P. T., Pan, W. L., Brooks, E. S., Huggins, and D. R., Lamb, B. K.: Carbon And Water Budgets In Multiple Wheat-Based Cropping Systems In The Inland Pacific Northwest Us: Comparison Of Cropsyst Simulations With Eddy Covariance Measurements, Frontiers In Ecology And Evolution, 5, 25-36, 2017a.
Chi, J., Waldo, S., Pressley, S. N., Russell, E. S., O'Keeffe, P. T., Pan, W. L., Huggins, D. R., Stöckle, C. O., Brooks, E. S., and Lamb, B. K.: Effects Of Climatic Conditions And Management Practices On Agricultural Carbon And Water Budgets In The Inland Pacific Northwest Usa, J. Geophys. Res. Atmos.: Biogeosciences, 122(12), 3142-3160, 2017b.
Chu, H., Baldocchi, D. D., Poindexter, C., Abraha, M., Desai, A. R., Bohrer, G., Arain, M. A., Griffis, T., Blanken, P. D., O'Halloran, T. L., Thomas, R. Q., Zhang, Q., Burns, S. P., Frank, J. M., Christian, D., Brown, S., Black, T. A., Gough, C. M., Law, B. E., Lee, X., Chen, J., Reed, D. E., Massman, W. J., Clark, K., Hatfield, J., Prueger, J., Bracho, R., Baker, J. M., and Martin, T. A.: Temporal Dynamics Of Aerodynamic Canopy Height Derived From Eddy Covariance Momentum Flux Data Across North American Flux Networks, Geophysical Research Letters, 45(5), 9275–9287, 2018.
Cleverly, J.: Ti Tree East OzFlux Site OzFlux: Australian and New Zealand Flux Research and Monitoring hdl: 102.100.100/14225, 2013.
Cleverly, J., Boulain, N., Villalobos-Vega, R., Grant, N., Faux, R., Wood, C., Cook, P. G., Yu, Q., Leigh, A., and Eamus, D.: Dynamics of component carbon fluxes in a semi-arid Acacia wood- land, central Australia, J. Geophys. Res.-Biogeo., 118, 1168–1185, 2013.
Conte, M. H., Weber, J. C., Carlson, P. J., Flanagan, L. B.: Molecular And Carbon Isotopic Composition Of Leaf Wax In Vegetation And Aerosols In A Northern Prairie Ecosystem, Oecologia, 135(1), 67-77, 2003.
Copernicus Climate Change Service (C3S): C3S ERA5-Land reanalysis. Copernicus Climate Change Service, (accessed on 11 October 2019), https://cds.climate.copernicus.eu/cdsapp#!/home, 2019.
Ershadi, A., McCabe, M. F., Evans, J. P., Chaney, N. W. and Wood, E. F.: Multi-site evaluation of terrestrial evaporation models using FLUXNET data, Agric. For. Meteorol., 187, 46–61, doi:10.1016/j.agrformet.2013.11.008, 2014.
Eugster, W., Rouse, W. R., Pielke Sr, R. A., Mcfadden, J. P., Baldocchi, D. D., Kittel, T. G. F., Chapin, F. S., Liston, G. E., Vidale, P. L., Vaganov, E. and Chambers, S.: Land-atmosphere energy exchange in Arctic tundra and boreal forest: available data and feedbacks to climate, Glob. Chang. Biol., 6(S1), 84–115, doi:10.1046/j.1365-2486.2000.06015.x, 2000.
Euskirchen, E. S., Bret-Harte, M. S., Shaver, G. R., Edgar, C. W., and Romanovsky, V. E.: Long-Term Release Of Carbon Dioxide From Arctic Tundra Ecosystems In Alaska, Ecosystems, 20(5), 960-974, 2017.
Ewenz, C.: Loxton OzFlux tower site OzFlux: Australian and New Zealand Flux Research and Monitoring hdl: 102.100.100/20838, 2015.
Galvagno, M., Wohlfahrt, G., Cremonese, E., Rossini, M., Colombo, R., Filippa, G., Julitta, T., Manca, G., Siniscalco, C., Morra di Cella, U. and Migliavacca, M.: Phenology and carbon dioxide source/sink strength of a subalpine grassland in response to an exceptionally short snow season, Environ. Res. Lett., 8, 025008, doi:10.1088/1748-9326/8/2/025008, 2013.
Gash, J. H. C. and Dolman, A. J.: Sonic anemometer (co)sine response and flux measurement I. The potential for (co)sine error to affect sonic anemometer-based flux measurements, Agric. For. Meteorol., 119, 195–207, doi:10.1016/S0168-1923(03)00137-0, 2003.
Gilmanov, T. G., Soussana, J. F., Aires, L., Allard, V., Ammann, C., Balzarolo, M., Barcza, Z., Bernhofer, C., Campbell, C. L., Cernusca, A., Cescatti, A., Clifton-Brown, J., Dirks, B. O. M., Dore, S., Eugster, W., Fuhrer, J., Gimeno, C., Gruenwald, T., Haszpra, L., Hensen, A., Ibrom, A., Jacobs, A. F. G., Jones, M. B., Lanigan, G., Laurila, T., Lohila, A., G.Manca, Marcolla, B., Nagy, Z., Pilegaard, K., Pinter, K., Pio, C., Raschi, A., Rogiers, N., Sanz, M. J., Stefani, P., Sutton, M., Tuba, Z., Valentini, R., Williams, M. L. and Wohlfahrt, G.: Partitioning European grassland net ecosystem CO2 exchange into gross primary productivity and ecosystem respiration using light response function analysis, Agric. Ecosyst. Environ., 121(1–2), 93–120, doi:10.1016/j.agee.2006.12.008, 2007.
Gilmanov, T. G., Aires, L., Barcza, Z., Baron, V. S., Belelli, L., Beringer, J., Billesbach, D., Bonal, D., Bradford, J., Ceschia, E., Cook, D., Corradi, C., Frank, A., Gianelle, D., Gimeno, C., Gruenwald, T., Guo, H., Hanan, N., Haszpra, L., Heilman, J., Jacobs, A., Jones, M. B., Johnson, D. A., Kiely, G., Li, S., Magliulo, V., Moors, E., Nagy, Z., Nasyrov, M., Owensby, C., Pinter, K., Pio, C., Reichstein, M., Sanz, M. J., Scott, R., Soussana, J. F., Stoy, P. C., Svejcar, T., Tuba, Z. and Zhou, G.: Productivity, Respiration, and Light-Response Parameters of World Grassland and Agroecosystems Derived From Flux-Tower Measurements, Rangel. Ecol. Manag., 63(1), 16–39, doi:10.2111/REM-D-09-00072.1, 2010.
Hilton, T. W., Davis, K. J. and Keller, K.: Evaluating terrestrial CO2 flux diagnoses and uncertainties from a simple land surface model and its residuals, Biogeosciences, 11, 217–235, doi:10.5194/bg-11-217-2014, 2014.
Hirano, T., Segah, H., Harada, T., Limin, S., June, T., Hirata, R. and Osaki, M.: Carbon dioxide balance of a tropical peat swamp forest in Kalimantan, Indonesia, Glob. Chang. Biol., 13(2), 412–425, doi:10.1111/j.1365-2486.2006.01301.x, 2007.

Hirata, R., Saigusa, N., Yamamoto, S., Ohtani, Y., Ide, R., Asanuma, J., Gamo, M., Hirano, T., Kondo, H., Kosugi, Y., Li, S. G., Nakai, Y., Takagi, K., Tani, M. and Wang, H.: Spatial distribution of carbon balance in forest ecosystems across East Asia, Agric. For. Meteorol., 148(5), 761–775, doi:10.1016/j.agrformet.2007.11.016, 2008.
Ikawa, H., Nakai, T., Busey, R., Kim, Y., Kobayashi, H., Nagai, S., Ueyama, M., Saito, K., Nagano, H., Suzuki, R. and Hinzman, L.: Understory CO2, sensible heat, and latent heat fluxes in a black spruce forest in interior Alaska, Agric. For. Meteorol., 214215, 80–90, 2015.
Irvine, J., Law, B. E. and Hibbard, K. A.: Postfire carbon pools and fluxes in semiarid ponderosa pine in Central Oregon, Glob. Chang. Biol., 13(8), 1748–1760, doi:10.1111/j.1365-2486.2007.01368.x, 2007.
King, M. D., Platnick, S., Moeller, C. C., Revercomb, H. E. and Chu, D. A.: Remote sensing of smoke, land, and clouds from the NASA ER-2 during SAFARI 2000, J. Geophys. Res. Atmos., 108(D13), doi:10.1029/2002JD003207, 2003.
Isaac P.: Daly Regrowth OzFlux tower site_old_20131128 OzFlux: Australian and New Zealand Flux Research and Monitoring hdl: 102.100.100/14215, 2010.
Jamali, H., Livesley, S. J., Dawes, T. Z., Cook, G. D., Hutley, L. B. and Arndt, S. K.: Diurnal and seasonal variations in CH4 flux from termite mounds in tropical savannas of the Northern Territory, Australia, Agric. For. Meteorol., 151(11), 1471–1479, doi:10.1016/j.agrformet.2010.06.009, 2011.
Keppel-Aleks, G., Wennberg, P. O., Washenfelder, R. A., Wunch, D., Schneider, T., Toon, G. C., Andres, R. J., Blavier, J.-F., Connor, B., Davis, K. J., Desai, A. R., Messerschmidt, J., Notholt, J., Roehl, C. M., Sherlock, V., Stephens, B. B., Vay, S. A., and Wofsy, S. C.: The imprint of surface fluxes and transport on variations in total column carbon dioxide, Biogeosciences, 9, 875–891, doi:10.5194/bg-9-875-2012, 2012.
Jung, M. et al.: FLUXCOM Global Land Energy Fluxes. Max Planck Institute for Biogeochemistry, Jena, (accessed on 2 October 2019), https://doi.org/10.17871/FLUXCOM_EnergyFluxes_v1 (2018)
Lafleur, P. M., Roulet, N. T., Bubier, J. L., Frolking, S. and Moore, T. R.: Interannual variability in the peatland-atmosphere carbon dioxide exchange at an ombrotrophic bog, Global Biogeochem. Cycles, 17(2), 1036, doi:10.1029/2002GB001983, 2003.
Laubach, J.: Beacon Farm OzFlux: Australian and New Zealand Flux Research and Monitoring hdl: 102.100.100/26730, 2016.
Li, X., Liang, S., Yu, G., Yuan, W., Cheng, X., Xia, J., Zhao, T., Feng, J., Ma, Z., Ma, M., Liu, S., Chen, J., Shao, C., Li, S., Zhang, X., Zhang, Z., Chen, S., Ohta, T., Varlagin, A., Miyata, A., Takagi, K., Saiqusa, N. and Kato, T.: Estimation of gross primary production over the terrestrial ecosystems in China, Ecol. Modell., 261–262, 80–92, doi:10.1016/j.ecolmodel.2013.03.024, 2013.
Liddell, M.: Cape Tribulation OzFlux tower site OzFlux: Australian and New Zealand Flux Research and Monitoring hdl: 102.100.100/14242, 2013a
Liddell, M.: Robson Creek OzFlux tower site OzFlux: Australian and New Zealand Flux Research and Monitoring hdl: 102.100.100/14243, 2013b.
Loubet, B., Laville, P., Lehuger, S., Larmanou, E., Fléchard, C., Mascher, N., Genermont, S., Roche, R., Ferrara, R. M., Stella, P., Personne, E., Durand, B., Decuq, C., Flura, D., Masson, S., Fanucci, O., Rampon, J.-N., Siemens, J., Kindler, R., Gabrielle, B., Schrumpf, M. and Cellier, P.: Carbon, nitrogen and Greenhouse gases budgets over a four years crop rotation in northern France, Plant Soil, 343(1–2), 109–137, doi:10.1007/s11104-011-0751-9, 2011.
Macfarlane, C.: Great Western Woodlands OzFlux: Australian and New Zealand Flux Research and Monitoring hdl: 102.100.100/14226, 2013.
McCaughey, J. H., Pejam, M. R., Arain, M. A., and Cameron, D. A.: Carbon dioxide and energy fluxes from a boreal mixedwood forest ecosystem in Ontario Canada, Agr. Forest Meteorol., 140, 79–96, 2006.
Mu, Q.: Mod16a2_monthly.Merra_gmao_1kmalb. (accessed on 1 October 2019), http://files.ntsg.umt.edu/data/NTSG_Products/MOD16/MOD16A2_MONTHLY.MERRA_GMAO_1kmALB/, 2015.
Noormets, A., Chen, J. and Crow, T. R.: Age-Dependent Changes in Ecosystem Carbon Fluxes in Managed Forests in Northern Wisconsin, USA, Ecosystems, 10(2), 187–203, doi:10.1007/s10021-007-9018-y, 2007.
ORNL DAAC: Home | fluxnetweb.ornl.gov, [online] Available from: https://fluxnet.ornl.gov/ (Accessed 1 July 2019), 2015.
Pendall E.: Cumberland Plain OzFlux Tower Site OzFlux: Australian and New Zealand Flux Research and Monitoring hdl: 102.100.100/25164, 2015.
Saleska, S.R., H.R. da Rocha, A.R. Huete, A.D. Nobre, P. Artaxo, and Y.E. Shimabukuro: . LBA-ECO CD-32 Flux Tower Network Data Compilation, Brazilian Amazon: 1999-2006. Data set. Available on-line [http://daac.ornl.gov] from Oak Ridge National Laboratory Distributed Active Archive Center, Oak Ridge, Tennessee, USA, doi:10.3334/ORNLDAAC/1174, 2013.
Reichstein, M., Rey, A., Freibauer, A., Tenhunen, J., Valentini, R., Banza, J., Casals, P., Cheng, Y., Grünzweig, J. M., Irvine, J., Joffre, R., Law, B. E., Loustau, D., Miglietta, F., Oechel, W., Ourcival, J.-M., Pereira, J. S., Peressotti, A., Ponti, F., Qi, Y., Rambal, S., Rayment, M., Romanya, J., Rossi, F., Tedeschi, V., Tirone, G., Xu, M. and Yakir, D.: Modeling temporal and large-scale spatial variability of soil respiration from soil water availability, temperature and vegetation productivity indices, Global Biogeochem. Cycles, 17(4), doi:10.1029/2003GB002035, 2003.
Reichstein, M., Falge, E., Baldocchi, D., Papale, D., Aubinet, M., Berbigier, P., Bernhofer, C., Buchmann, N., Gilmanov, T., Granier, A., Grunwald, T., Havrankova, K., Ilvesniemi, H., Janous, D., Knohl, A., Laurila, T., Lohila, A., Loustau, D., Matteucci, G., Meyers, T., Miglietta, F., Ourcival, J.-M., Pumpanen, J., Rambal, S., Rotenberg, E., Sanz, M., Tenhunen, J., Seufert, G., Vaccari, F., Vesala,

T., Yakir, D. and Valentini, R.: On the separation of net ecosystem exchange into assimilation and ecosystem respiration: review and improved algorithm, Glob. Chang. Biol., 11(9), 1424–1439, doi:10.1111/j.1365-2486.2005.001002.x, 2005.
Revill, A., Sus, O., Barrett, B. and Williams, M.: Carbon cycling of European croplands: A framework for the assimilation of optical and microwave Earth observation data, Remote Sens. Environ., 137, 84–93, doi:10.1016/j.rse.2013.06.002, 2013.
Schroder, I.: Arcturus Emerald OzFlux tower site OzFlux: Australian and New Zealand Flux Research and Monitoring hdl: 102.100.100/14249, 2014.
Silberstein, R: Gingin OzFlux, Australian and New Zealand Flux Research and Monitoring hdl: 102.100.100/22677, 2015.
Soegaard, H. and Nordstroem, C.: Carbon dioxide exchange in a high-arctic fen estimated by eddy covariance measurements and modelling, Glob. Chang. Biol., 5(5), 547–562, doi:10.1111/j.1365-2486.1999.00250.x, 1999.
Stoy, P. C., Mauder, M., Foken, T., Marcolla, B., Boegh, E., Ibrom, A., Arain, M. A., Arneth, A., Aurela, M., Bernhofer, C., Cescatti, A., Dellwik, E., Duce, P., Gianelle, D., van Gorsel, E., Kiely, G., Knohl, A., Margolis, H., Mccaughey, H., Merbold, L., Montagnani, L., Papale, D., Reichstein, M., Saunders, M., Serrano-Ortiz, P., Sottocornola, M., Spano, D., Vaccari, F. and Varlagin, A.: A data-driven analysis of energy balance closure across FLUXNET research sites: The role of landscape scale heterogeneity, Agric. For. Meteorol., 171–172, 137–152, doi:10.1016/j.agrformet.2012.11.004, 2013.
Stefan A.: Wombat State Forest OzFlux-tower site OzFlux: Australian and New Zealand Flux Research and Monitoring hdl: 102.100.100/14237, 2013.
Sulkava, M., Luyssaert, S., Zaehle, S. and Papale, D.: Assessing and improving the representativeness of monitoring networks: The European flux tower network example, J. Geophys. Res., 116(G3), G00J04, doi:10.1029/2010JG001562, 2011.
Wei, S., Yi, C., Hendrey, G., Eaton, T., Rustic, G., Wang, S., Liu, H., Krakauer, N. Y., Wang, W., Desai, A. R., Montagnani, L., Tha Paw U, K., Falk, M., Black, A., Bernhofer, C., Grünwald, T., Laurila, T., Cescatti, A., Moors, E., Bracho, R. and Valentini, R.: Data-based perfect-deficit approach to understanding climate extremes and forest carbon assimilation capacity, Environ. Res. Lett., 9, 065002, doi:10.1088/1748-9326/9/6/065002, 2014.
Wood, E.: Princeton University SRB/GEWEX evapotranspiration (Penman-Monteith) L4 3 hour 0.5 degree x 0.5 degree V1, Greenbelt, MD USA, Goddard Earth Sciences Data and Information Services Center (GES DISC), (accessed on 1 October 2019), 10.5067/MEASURES/WATERCYCLE/DATA314, 2017
Woodgate, W.: Tumbarumba OzFlux tower site OzFlux: Australian and New Zealand Flux Research and Monitoring hdl: 102.100.100/14241, 2013.
Zhang, Y., Pena A. J., McVicar, T. Chiew, F.; Vaze, J., Zheng, H., Wang, Y.: Monthly global observation-driven Penman-Monteith-Leuning (PML) evapotranspiration and components. v2. CSIRO. Data Collection. (accessed on 9 April 2019), https://doi.org/10.4225/08/5719A5C48DB85, 2016.
Zhang, Ke: PLSH Monthly Global 8kmResolution: (accessed on 30 September 2019), http://files.ntsg.umt.edu/data/ET_global_monthly/Global_8kmResolution/, 2017.